ACS Macro Letters

Letter

pubs.acs.org/macroletters

Controlled Nanopores by Supramolecular Assembly of End-Functionalized Dendrimer and Homopolymer Blend

Giyoung Song,[†,‡] Ju Eun Kim,[‡,§] Suk Man Cho,[†] Seong Ik Jeon,[§] Hui Joon Park,[∥] June Huh,[⊥] Cheol-Hee Ahn,*[,§] and Cheolmin Park*[,†]

[†]Department of Materials Science and Engineering, Yonsei University, Seoul, 120-749, Korea

[§]Department of Materials Science and Engineering, Seoul University, San 56-1, Gwanak_599 Gwanak-ro, Seoul, 515-744, Korea

[∥]Division of Energy Systems Research, Ajou University, 206 World cup-ro, Suwon 443-749, Korea

[⊥]Department of Chemical and Biological Engineering, Korea University, Anam-dong, Seongbuk-gu, Seoul 136-713, Korea

Supporting Information

ABSTRACT: Supramolecular assembly of end-functionalized polymers, forming block copolymer-like supramolecules based on ionic interaction, has been utilized as a simple and facile method for generating functionalized nanoporous thin film. Here, the binary blend film of aminated poly(ethylene oxide) dendrimer (APEO-G) and sulfonated polystyrene (SPS) at a stoichiometric composition after benzene/water solvent vapor annealing exhibits spherical domains in multilayers over a large area. By controlling the number of end-functional arms of dendrimer via divergent ring-opening polymerization of ethylene oxide as well as the molecular weights of SPS, the domain sizes can be controlled ranging from mainly 34 to 54 nm, even to 131 nm. Our supramolecular-assembly system provides an alternative approach to fabricating a functional nanotemplate by easily etching domains with selective solvent treatment and leaving functional groups at the pore surfaces.

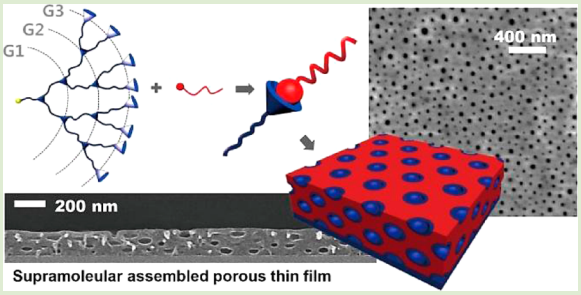

Interests in nanoporous structures have been continuously increased due to their potential applications to sensing,[1] separating,[2] and templating.[3] Among various approaches to access those nanoscale morphologies, self-assembled nanostructures from biopolymers,[4] surfactants,[5] nanoparticles,[6] and amphiphilic block copolymers,[7,8] which are advantageous to a variety of structures formation and tunability, have been recognized as promising candidates for the fabrication of those nanoscale structures. However, laborious efforts are often needed in the fabrication procedures such as high energy consumption (e.g., UV and ozone)[9] or complicated chemical processes (e.g., etching).[10] In addition, the limitation of material selection or the necessity of additional processes[11] is required to control the surface functionality of structures, which hampers the ability to make these approaches universal.

Recently, it has been shown that the specific interactions, such as ionic interaction,[12−15] hydrogen bond[16−18] and halogen bond-driven self-assembly[19] between functional groups were introduced at the end of thermodynamically unfavorable polymer blends and they were utilized to form supramolecular complexes, ultimately giving rise to diverse self-assembled nanoscale morphologies. Different from the conventional block copolymer system, those nanostructures have unique properties such as easy cleavability of the linkage between polymer blocks, which is advantageous to form porous structures. Moreover, functional groups left on the surface of porous structures after removing one domain can be potential active sites for additional functionality of the structures.

Previously, we have demonstrated that those supramolecular systems were utilized to generate nanoporous templates in thin film condition.[15] A binary blend system, composed of monosulfonated polystyrene (SPS) and monoaminated poly(ethylene oxide) (APEO), was studied, and the surface functionalized nanoporous structures were successfully formed at a stoichiometric SPS weight fraction, $\Phi_{st} \approx 0.7$ in which the number of functional groups of both components are the same, through the ionic interaction between proton-donating sulfonic acid group and proton-accepting amino group. However, the difficulty in controlling their nanoscale morphologies still remained as an issue. To overcome this limitation, here, we report domain size-tunable nanoporous templates, based on utilizing the supramolecular assembly of end-functionalized dendrimer with multiarms and homopolymer. By controlling the number of end-functional groups of dendrimers, as well as the molecular weight of homopolymers, the domain size of thin nanoporous template films, evolved in combination with the benzene/water cosolvent vapor annealing, could be successfully controlled. Our results suggest that the end-functionalized polymer blend system having multiple ionic bonding sites can

Received: August 8, 2014
Accepted: October 7, 2014
Published: October 14, 2014

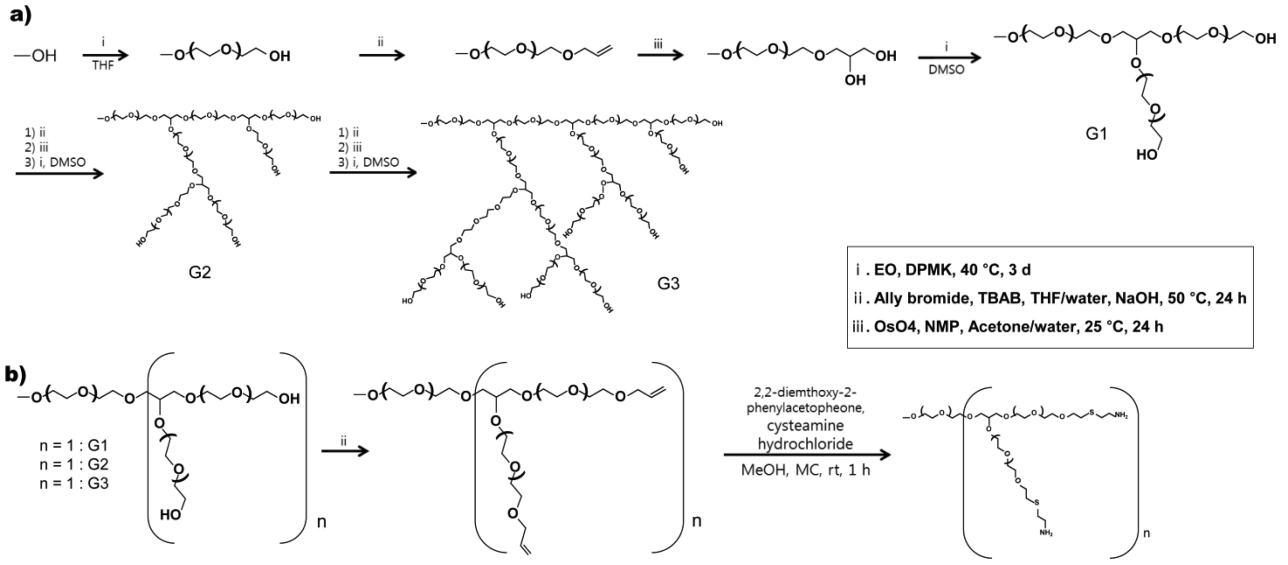

Figure 1. (a) Anionic ring-opening polymerization of G1, G2, and G3 dendrimers; (b) Introduction of amine group to branch point of G1, G2, and G3 dendrimers.

be a promising approach to achieve domain-size tunable multileveled nanoporous thin film.

Our approach is primarily based on the supramolecular assembly that arises from the ionic interaction between functional groups of the end-functionalized unfavorable polymer chains, proton-donating monoend sulfonated polystyrene (SPS) and proton-accepting multiend aminated poly(ethylene oxide) dendrimer (APEO-G). The competition between the repulsion of the unfavorable polymer blocks, PS and PEO, and the attraction of end-to-end ionic interaction consequently induces the supramolecular assembled nanostructures. Additionally, to control the domain sizes of those nanostructures, APEO is modified to the dendrimer type branched macromolecule that can have multiple interacting sites. APEO dendrimers were synthesized using anionic ring-opening polymerization of ethylene oxide (EO) as schematically shown in Figure 1. Polymerization was carried out in THF with the introduction of EO to produce linear PEO (G0). In order to introduce dihydroxylated branch points at the end of G0, the polymer was subsequently reacted with allyl bromide and then osmium tetroxide. Higher generation dendrimers were obtained using the same growth and activation steps, repeating living anionic polymerization, allylation, and dihydroxylation, as shown in Figure 1a. Figure 1b illustrates the amino group functionalization at the focal point of each dendrimer using cysteamine hydrochloride. Molecular weight and polydispersity of the dendrimers were obtained using GPC (Supporting Information S1). ^{1}H NMR analysis confirmed the allylation, dihydroxylation, and amine functionalization steps (Supporting Information S2).

Those multiend-aminated PEO dendrimers are denoted as APEO-G1, APEO-G2, and APEO-G3 according to the generation, which means the number of repeated branching cycles during their synthesis. For instance, APEO-G1, APEO-G2, and APEO-G3 have 2, 4, and 8 functional groups, respectively, as schematically depicted in Figure 2. The molecular weight of SPS was also adjusted as another parameter to control the domain size of the structures. The blend samples were prepared by spin-casting 2 wt % solution of APEO-G and SPS dissolved in benzene on a Si wafer and the subsequent

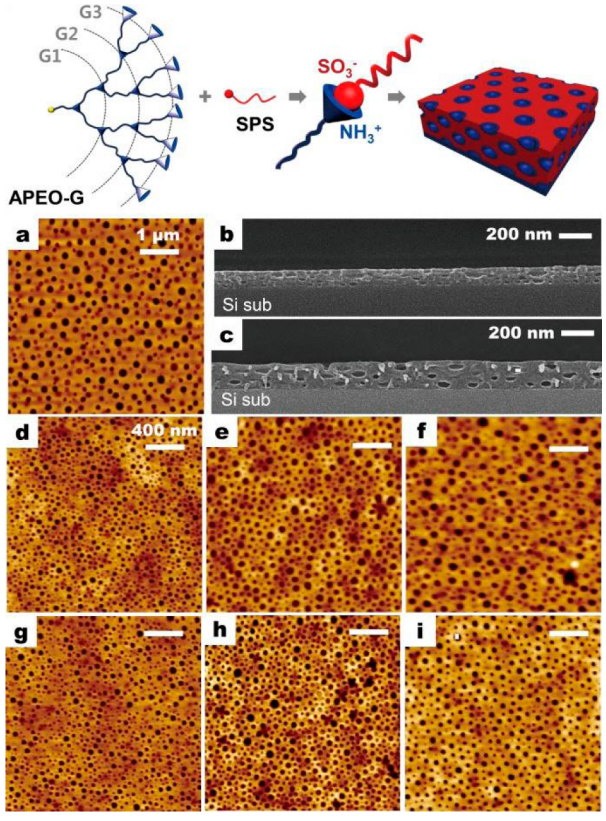

Figure 2. Schematic and TM-AFM images in height contrast of (a) APEO-G1/SPS3, (d) APEO-G2/SPS1, (e) APEO-G2/SPS2, (f) APEO-G2/SPS3, (g) APEO-G3/SPS1, (h) APEO-G3/SPS2, and (i) APEO-G3/SPS3. SEM images of cross sectional films of (b) APEO-G2/SPS2 and (c) APEO-G2/SPS3.

solvent annealing under the vapor of benzene/water mixture.[20] An optimized benzene to water ratio (v/v, 8:2) was used to obtain the best structural ordering, as explained in our previous study.[15] The nine different types of samples, the combinations of three different APEO-Gs (APEO-G1, APEO-G2, APEO-G3) and three different SPSs (SPS1, SPS2 and SPS3), were

dx.doi.org/10.1021/mz500484k | ACS Macro Lett. 2014, 3, 1112−1116

prepared, and their stoichiometric SPS weight fractions (Φ_{st}) were set to be approximately 0.5, 0.62 and 0.75, corresponding to the SPS1, SPS2, and SPS3-based blend samples, respectively (Table 1).

Table 1. SPS Stoichiometric Ratios with SPS and Dendrimer APEO-G Compositions

	SPS1 (10.5 kg mol^{-1})	SPS2 (17 kg mol^{-1})	SPS3 (31.5 kg mol^{-1})
APEO-G1 (21 kg mol^{-1})	$Ø_{SPS}$ = 0.50	$Ø_{SPS}$ = 0.62	$Ø_{SPS}$ = 0.75
APEO-G2 (43 kg mol^{-1})	$Ø_{SPS}$ = 0.49	$Ø_{SPS}$ = 0.61	$Ø_{SPS}$ = 0.75
APEO-G3 (78 kg mol^{-1})	$Ø_{SPS}$ = 0.52	$Ø_{SPS}$ = 0.64	$Ø_{SPS}$ = 0.76

As shown in the tapping-mode atomic force microscopy (TM-AFM) images of the polymer blend films, treated by solvent vapor annealing, spherical-shape nanoporous domain arrays are well-formed over the whole area of the film (Figure 2). Our previous study revealed that benzene vapor plays a major role in the formation of nanostructures by the organization of SPS and APEO polymer chains, and water vapor induces the formation of the nanopores in the structures.[15] Water vapor migrates into the APEO domains or in the SPS/APEO interface during the solvent annealing, which lowers not only the polymer density in APEO domains, but also weakens the end-to-end ionic interaction ($NH_3^+\cdots SO_3^-$). In this circumstance, the PEO chains tend to collapse to reduce PEO/air contacts, giving rise to pores in the PEO domain rather than PS matrix. It should be noted, however, that the large configurational entropy due to the small molecular size of water leads to the broad distributions of water molecules in the PEO domains, which contributes to the wide distributions of pore size. Our cross-sectional FE-SEM images (Figure 2b,c) also show that the multilayered nanopore structures are successfully generated in our blend samples.

Notably, the SEM images (Figure 2b,c) clearly indicate that pores are more like prolate spheroid rather than sphere. Given that the water evaporation proceeds from the top of each PEO domain sequentially to the larger depth in the domain, the chain collapse of PEO also occurs sequentially such that PEO segments are piled up more in the depth direction than in the lateral direction in order to avoid air whose contact line is going down from the top. This anisotropic PEO collapse results in the prolate spherical pore instead of the spherical pore.

Interestingly, more detailed analysis of the morphologies of six pairs of our supramolecular blended films in Figure 3a shows that we can also control the domain size of nanoporous structures using our dendrimer-based supramolecular assembly. To elucidate the factors that can affect the domain size of nanostructures, the correlation between the diameter of nanopores of specific APEO-G/SPS polymer pairs and their blend compositions was analyzed using their AFM images. For this purpose, the pore diameter distributions from several sets of AFM images were calculated by *ImageJ* program (Supporting Information S3).

Our results showed that the largest pores of approximately 131 nm in diameter were obtained from the APEO-G1/SPS3 pair among all the other APEO-G2- and APEO-G3-based samples. In addition, the average pore diameters of APEO-G2-based samples increase from 35.9 to 53.8 nm as the molecular weight of the counter SPS increases (SP1 → SP2 → SP3), and

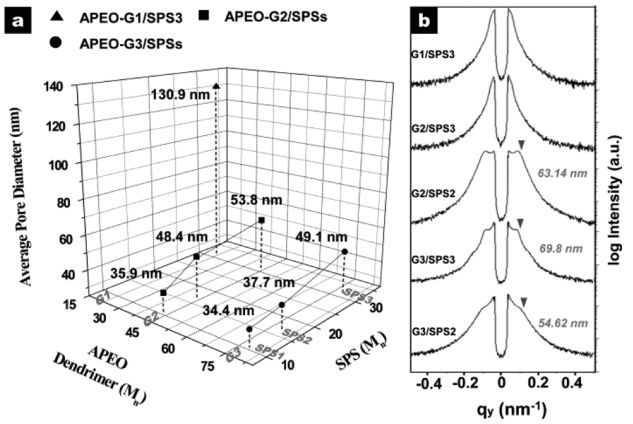

Figure 3. Average pore diameters (z) were transposed onto the graph with the plots of molecular weight of APEO-G dendrimers (x) and SPSs (y). The supramolecular assembly of end-functionalized dendrimer and homopolymer blends allowed for control of domain sizes ranging from approximately 34 to 131 nm. (b) 1D-GISAXS patterns of circular nanopores of blend films, showing the strong first-order reflection at an in-plane scattering vector, q_{xy}, of approximately 0.0995, 0.0890, and 0.115 nm^{-1} for APEO-G2/SPS2, APEO-G3/SPS3, and G3/SPS2, respectively. No reflection peaks were observed from APEO-G1/SPS3 and APEO-G2/SPS3 films due to the large nanostructures of the films.

those of APEO-G3-based samples increase from 34.4 to 49.1 nm as the molecular weight of counter SPS increases (SP1 → SP2 → SP3). We can see that domain size can be controlled by adjusting the molecular weight of SPSs in a given APEO-G system.

Grazing incident small-angle X-ray scattering (GISAXS) confirms the domain spacing variations as representative 1D line profiles of the 2D GISAXS patterns of blend films (Supporting Information S4) shown in Figure 3b. The first strong reflection peaks from APEO-G2/SPS2, APEO-G3/SPS3, and SPS2 indicate that the characteristic distances are approximately 63.1, 69.8, and 54.6 nm, which correspond to the (100) planes of hexagonally packed nanodomains. Unfortunately, no reflections were observed from APEO-G1/SPS3 and APEO-G2/SPS3 due to the large domain structures of the films.

The variation of pore size observed may be due to the difference in the number of supramolecular end-functional interactions with the molecular weight of SPS. The formation of supramolecules by the interaction between the two functional groups at the end of the PEO and PS polymer chains depends on a molecular parameter $\kappa = -f_b(N\chi K_B T)^{-1}$, where f_b is the free energy change of end-association of a single bond, χ is the Flory–Huggins parameter about the immiscibility between different polymer blocks, and N is the degree of polymerization. When the parameter κ is larger than a critical value κ_c ($\kappa > \kappa_c$), the chain end interaction is strong enough to form a block copolymer-like supramolecular assembly.[14,15] Therefore, when a given dendrimer is combined with a higher molecular weight SPS that leads to an increase in N, the number of supramolecular end-functional interactions becomes less. Consequently, one can expect that the unbound APEO-G and SPS homopolymers are distributed to the APEO-G-rich spherical domain and SPS-rich matrix, respectively. This makes both PEO and PS domains swollen during the solvent annealing.[21] As shown in Figure 2d–f for APEO-G2/SPSs and Figure 2g–i for APEO-G3/SPSs, both size of nanodomains

dx.doi.org/10.1021/mz500484k | *ACS Macro Lett.* 2014, 3, 1112–1116

and the sphere-to-sphere distances increase with the molecular weight of SPS (Supporting Information S3).

The nanodomains were further controlled by changing the functionality of polymer chains with dendrimer system. Our supramolecular systems having the same stoichiometric compositions between PEO and PS (e.g., APEO-G1/SPS3, APEO-G2/SPS3, and APEO-G3/SPS3 for ~0.75 Φ_{st}, APEO-G2/SPS2 and APEO-G3/SPS2 for ~0.6 Φ_{st}, and APEO-G2/SPS1 and APEO-G3/SPS1 for ~0.5 Φ_{st}) allowed us to reduce the size of nanofeatures by increasing the number of end-functionality of APEO-G molecules with the increased generation of the dendrimers (Figure 3). The concentrations of both unbound SPS and APEO would decrease with the number of dendrimer arms due to the enhanced binding force per dendrimer molecule with generation. Subsequently, the less amount of unbound polymers with the higher generation dendrimer rendered both pore and interpore distance smaller.

Furthermore, two phases from macro-phase separations (Supporting Information S5), shown in APEO-G1/SPS1 at ~0.5 Φ_{st} and APEO-G1/SPS2 at ~0.6 Φ_{st}, were successfully suppressed by just increasing the chain-end functionality with dendrimers having higher generations even at the same stoichiometric compositions (e.g., APEO-G2/SPS1 and APEO-G3/SPS1 at ~0.5 Φ_{st}, and APEO-G2/SPS2 and APEO-G3/SPS2 at ~0.6 Φ_{st}), giving rise to characteristic microphase-separated morphologies. The blend films obtained from the low concentrated solutions (e.g., 1 wt %) show the partially covered film morphologies (Supporting Information S6).

Our approach serves a simple and convenient method for fabricating the thin surface-functionalized nanoporous films. Because the noncovalent bonding between the two different polymers, based on end-to-end ionic interaction ($NH_3^+\cdots SO_3^-$), can be easily cleaved by solvent treatment, we were able to readily eliminate the APEO-G domains with the selective solvent to PEO domains such as ethanol. Figure 4a,b clearly shows that the pores became larger after the etching process. The elimination of PEO molecules was confirmed by XPS, in which the intensities of oxygen electron emission, detected at 533 eV, decrease significantly as shown in Figure 4c. It is expected that the SO_3^- groups left on the surface of nanopores can be further utilized as functional active sites for further applications.

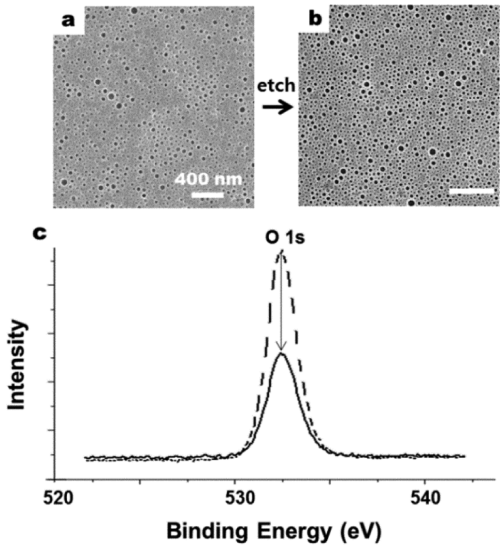

Figure 4. SEM images of solvent annealed films of (a) APEO-G3/SPS2 and (b) the film etched with domains by ethanol. (c) The XPS spectra of oxygen peaks of APEO-G3/SPS2 films before (dotted line) and after (solid line) the etching step.

In conclusion, we demonstrated the supramolecular-assembled nanoporous thin films based on the ionic interaction of the end-functionalized dendrimer (multiend aminated poly(ethylene oxide), APEO-G) and the homopolymer (monoend sulfonated polystyrene, SPS) mixture. The nanoporous thin films from two polymer blends were readily obtained by benzene/water cosolvent annealing in which easy cleavage of the ionic bonds occurred and APEO molecules were selectively removed.

More interestingly, by controlling the functionality of polymer chains for the ionic interaction with the dendrimer system and changing the molecular weight of polymers, the domain size was tunable. Our supramolecular assembly system has a further advantage of easy introduction of the functional active sites to the pore surfaces by simple solvent etching for the chemically active polymer nanotemplate.

■ ASSOCIATED CONTENT

Supporting Information

Experimental section, characterization, and Figures S1−S6. This material is available free of charge via the Internet at http://pubs.acs.org.

■ AUTHOR INFORMATION

Corresponding Authors

*E-mail: chahn@snu.ac.kr.

* E-mail:cmpark@yonsei.ac.kr.

Author Contributions

‡These authors contributed equally (G.S. and J.E.K.).

Notes

The authors declare no competing financial interest.

■ ACKNOWLEDGMENTS

This study was supported by the National Research Foundation of Korea (NRF) grant funded by the Korea government (MEST; No.2014R1A2A1A01005046) and the Pioneer Research Center Program through the National Research Foundation of Korea funded by the Ministry of Science, ICT and Future Planning (2010-0019313). This research was also supported by the third stage of Brain Korea 21 Plus Project in 2014 and the X-ray experiments at PAL (3C, beamline), Korea, were supported by MEST and POSCO, Korea.

■ REFERENCES

(1) Lang, X.-Y.; Fu, H.-Y.; Hou, C.; Han, G.-F.; Yang, P.; Liu, Y.-B.; Jiang, Q. *Nat. Commun.* **2013**, *4*, 1−8.

(2) Li, H.; Song, Z.; Zhang, X.; Huang, Y.; Li, S.; Mao, Y.; Ploehn, H. J.; Bao, Y.; Yu, M. *Science* **2013**, *342*, 95−98.

(3) Zavala-Rivera, P.; Channon, K.; Nguyen, V.; Sivaniah, E.; Kabra, D.; Friend, R. H.; Nataraj, S. K.; Al-Muhtaseb, S. A.; Hexemer, A.; Calvo, M. E.; Miguez, H. *Nat. Mater.* **2012**, *11*, 53−57.

(4) Du, C.; Falini, G.; Fermani, S.; Abbott, C.; Moradian-Oldak, J. *Science* **2005**, *307*, 1450−1454.

(5) Meng, Y.; Gu, D.; Zhang, F.; Shi, Y.; Yang, H.; Li, Z.; Yu, C.; Tu, B.; Zhao, D. *Angew. Chem., Int. Ed.* **2005**, *117*, 7215−7221.

(6) Acharya, H.; Sung, J.; Sohn, B.-H.; Kim, D. H.; Tamada, K.; Park, C. *Chem. Mater.* **2009**, *21*, 4248−4255.

(7) Gu, W.; Huh, J.; Hong, S. W.; Sveinbjornsson, B. R.; Park, C.; Grubbs, R. H.; Russell, T. P. *ACS Nano* **2013**, *7*, 2551−2558.
(8) Kim, E.; Ahn, H.; Park, S.; Lee, H.; Lee, M.; Lee, S.; Kim, T.; Kwak, E.-A.; Lee, J. H.; Lei, X.; Huh, J.; Bang, J.; Lee, B.; Ryu, D. Y. *ACS Nano* **2013**, *7*, 1952−1960.
(9) Park, C.; Yoon, J.; Thomas, E. L. *Polymer* **2003**, *44*, 6725−6760.
(10) Zhao, D.; Feng, J.; Huo, Q.; Melosh, N.; Fredrickson, G. H.; Chmelka, B. F.; Stucky, G. D. *Science* **1998**, *279*, 548−552.
(11) Feng, X.; Fryxell, G. E.; Wang, L.-Q.; Kim, A. Y.; Liu, J.; Kemner, K. M. *Science* **1997**, *276*, 923−926.
(12) Russell, T. P.; Jerome, R.; Charlier, P.; Foucart, M. *Macromolecules* **1988**, *21*, 1709−1717.
(13) Huh, J.; Jo, W. H. *Macromolecules* **2004**, *37*, 3037−3048.
(14) Huh, J.; Jung, J. Y.; Lee, J. U.; Cho, H.; Park, S.; Park, C.; Jo, W. H. *ACS Nano* **2010**, *5*, 115−122.
(15) Song, G.; Cho, S. M.; Jung, H. J.; Kim, R. H.; Bae, I.; Ahn, H.; Ryu, D. Y.; Huh, J.; Park, C. *Chem.—Eur. J.* **2012**, *18*, 15662−15668.
(16) Huh, J.; Ikkala, O.; ten Brinke, G. *Macromolecules* **1997**, *30*, 1828−1835.
(17) Ruokolainen, J.; Mäkinen, R.; Torkkeli, M.; Mäkelä, T.; Serimaa, R.; Brinke, G. t.; Ikkala, O. *Science* **1998**, *280*, 557−560.
(18) Tang, C.; Lennon, E. M.; Fredrickson, G. H.; Kramer, E. J.; Hawker, C. J. *Science* **2008**, *322*, 429−432.
(19) Houbenov, N.; Milani, R.; Poutanen, M.; Haataja, J.; Dichiarante, V.; Sainio, J.; Ruokolainen, J.; Resnati, G.; Metrangolo, P.; Ikkala, O. *Nat. Commun.* **2014**, *5*, 1−8.
(20) Kim, T. H.; Huh, J.; Park, C. *Macromolecules* **2010**, *43*, 5352−5357.
(21) Matsen, M. W. *Macromolecules* **1995**, *28*, 5765−5773.